



OPEN ACCESS

EDITED BY

William Raoul,
Croissance et Cancer, France

REVIEWED BY

Miguel Pereira-Silva,
University of Coimbra, Portugal
Jean-Michel Escoffre,
INSERM U1253 Imagerie et Cerveau
(iBrain), France

*CORRESPONDENCE

Nosratollah Zarghami,
✉ zarghami@tbzmed.ac.ir

†These authors have contributed equally
to this work

RECEIVED 25 February 2023

ACCEPTED 23 May 2023

PUBLISHED 27 June 2023

CITATION

Shafiei G, Jafari-Gharabaghlu D,
Farhoudi-Sefidan-Jadid M, Alizadeh E,
Fathi M and Zarghami N (2023), Targeted
delivery of silibinin via magnetic niosomal
nanoparticles: potential application in
treatment of colon cancer cells.
Front. Pharmacol. 14:1174120.
doi: 10.3389/fphar.2023.1174120

COPYRIGHT

© 2023 Shafiei, Jafari-Gharabaghlu,
Farhoudi-Sefidan-Jadid, Alizadeh, Fathi
and Zarghami. This is an open-access
article distributed under the terms of the
[Creative Commons Attribution License
\(CC BY\)](https://creativecommons.org/licenses/by/4.0/). The use, distribution or
reproduction in other forums is
permitted, provided the original author(s)
and the copyright owner(s) are credited
and that the original publication in this
journal is cited, in accordance with
accepted academic practice. No use,
distribution or reproduction is permitted
which does not comply with these terms.

Targeted delivery of silibinin via magnetic niosomal nanoparticles: potential application in treatment of colon cancer cells

Golchin Shafiei^{1,2†}, Davoud Jafari-Gharabaghlu^{3†},
Mahdi Farhoudi-Sefidan-Jadid³, Effat Alizadeh¹, Marziyeh Fathi²
and Nosratollah Zarghami^{3,4*}

¹Department of Medical Biotechnology, Faculty of Advanced Medical Sciences, Tabriz University of Medical Sciences, Tabriz, Iran, ²Research Center for Pharmaceutical Nanotechnology, Biomedicine Institute, Tabriz University of Medical Sciences, Tabriz, Iran, ³Department of Clinical Biochemistry and Laboratory Medicine, Faculty of Medicine, Tabriz University of Medical Sciences, Tabriz, Iran, ⁴Department of Medical Biochemistry, Faculty of Medicine, Istanbul Aydin University, Istanbul, Turkey

Introduction: In recent years, various nanoparticles (NPs) have been discovered and synthesized for the targeted therapy of cancer cells. Targeted delivery increases the local concentration of therapeutics and minimizes side effects. Therefore, NPs-mediated targeted drug delivery systems have become a promising approach for the treatment of various cancers. As a result, in the current study, we aimed to design silibinin-loaded magnetic niosomes nanoparticles (MNNPs) and investigate their cytotoxicity property in colorectal cancer cell treatment.

Methods: MNNPs ferrofluids were prepared and encapsulated into niosomes (NIOs) by the thin film hydration method. Afterward, the morphology, size, and chemical structure of the synthesized MNNPs were evaluated using the TEM, DLS, and FT-IR techniques, respectively.

Results and Discussion: The distribution number of MNNPs was obtained at about 50 nm and 70 nm with a surface charge of -19.0 mV by TEM and DLS analysis, respectively. Silibinin loading efficiency in NIOs was about 90%, and the drug release pattern showed a controlled release with a maximum amount of about 49% and 70%, within 4 h in pH = 7.4 and pH = 5.8, respectively. To investigate the cytotoxicity effect, HT-29 cells were treated with the various concentration of the drugs for 24 and 48 h and evaluated by the MTT as well as flow cytometry assays. Obtained results demonstrated promoted cell cytotoxicity of silibinin-loaded MNNPs (5-fold decrease in cell viability) compared to pure silibinin (3-fold decrease in cell viability) while had no significant cytotoxic effect on HEK-293 (normal cell line) cells, and the cellular uptake level of MNNPs by the HT-29 cell line was enhanced compared to the control group. In conclusion, silibinin-loaded MNNPs complex can be considered as an efficient treatment approach for colorectal cancer cells.

KEYWORDS

silibinin, niosome, targeted therapy, magnetic nanoparticle, drug delivery, colon cancer

Introduction

Generally, cancer is a disorder in which abnormal cells are reinforced by escaping the conventional regulations of cellular division (Soltanian and Matin, 2011). Millions of people are being suffered from cancer, and the mortality caused by different kinds of cancer is dramatically growing in the world. Only in the United States, 1.7 million new cases of cancer were reported and over half a million people died of cancer in 2019, according to the Center for Disease Control (CDC) report (Hulvat, 2020). By 2029, it is estimated that there will be 16.8 million cancer deaths and 25.5 million new cancer cases annually (Thun et al., 2010). Colorectal cancer (CRC) is one of the most common malignancies in the digestive system, and it has been reported as the third most common malignant tumor worldwide (O'Leary et al., 2018). The occurrence of CRC is expanding in metropolitan regions and industrialized nations, as well as nations encountering financial change, like Eastern Europe, most Asian nations, and a few South American nations (Bray et al., 2018). According to a recent study in Iran, the prevalence of CRC caused by adenomatous polyps (the most common cause) is about 34%, which is almost equal to the rate reported in developed countries. Targeted drug delivery for the pathogenesis factors of CRC has become an advance, and the recruitment of nanotechnology approaches has opened new horizons in this area (Tiwari et al., 2020).

Each cancer treatment method has benefits and disadvantages, and combined treatment is vital to get the best results (Mohammadian et al., 2016a; Mokhtari et al., 2017; Hassani et al., 2022). Since more than 85% of human cancers are solid tumors, current cancer therapy techniques usually contain invasive procedures, like chemotherapy, to shrink tumors before surgical removal (Rolston, 2017). Chemotherapy drugs target rapidly dividing cells, which are property of most types of cancer cells and some normal tissues. Although cytotoxic cancer drugs are highly effective, they exhibit significant adverse effects that limit the dose of chemotherapy drugs (Pérez-Herrero and Fernández-Medarde, 2015; Alagheband et al., 2022). Problems associated with chemotherapy are drug non-specificity caused by poor drug delivery systems. These problems are being solved using nanoparticles (NPs) as drug delivery systems (DDSs) or nanocarriers like protein cages, liposomes, micelles, niosomes (NIOs), metal, polymer, and protein NPs (Jadid et al., 2023; Jafari-Gharabaghloou et al., 2023). NIOs are a type of NPs used in drug delivery and consist of layered structures of vesicles made from non-ionic surfactants. NIOs are carriers of a hydrophobic and hydrophilic anticancer drug because they have an amphiphilic property, and can increase the half-life of the drugs conjugated with NPs in cancer cells (Coviello et al., 2015; Eatemadi et al., 2016). Owing to their lower toxicity, they improve the therapeutic index by limiting the drug action to the target cells. The non-ionic surfactant in NIOs is biodegradable and biocompatible, thus does not stimulate the body's immune system (Liu et al., 2017). Moreover, there is no need to manage and store surfactants in a specific condition. To boost the DDS function, a localized magnetic field is applied to direct the aggregation of NIOs in the target (Liu et al., 2017). Recently, magnetic NIOs NPs (MNNPs) conjugated with anticancer drugs are investigated. Promising results are reported about stimulus-responsive drug release at the target cancer site by applying an

external magnetic field (Jamshidifar et al., 2021; Maurer et al., 2021; Momekova et al., 2021; Salmani Javan et al., 2022). The role of MNPs in bio-medicine, especially in the field of drug delivery, is important because their inherent magnetism facilitates many tasks, including targeting, which is very important and necessary in drug delivery (Mou et al., 2015). The combination of NIOs and MNPs provides both carrier targeting as well as drug protection properties that can be used as an efficient system for drug delivery (Pardakhty1 and Moazeni, 2013). Metal NPs can be enclosed inside NIOs with the desired drug to form MNNPs. Within the last decades, studies have focused on magnetic delivery approaches for vesicular DDSs, however, MNNPs have not been investigated widely. Plant-based drugs are usually the extract of medicinal herbs with different therapeutic applications (Solowey et al., 2014). Within the past decades, researchers have focused on herbal extracts, because of their anticancer and anti-neoplastic properties. Silibinin is an extract obtained from the medicinal plant *Silybum marianum* (Valková et al., 2021). Silibinin is the most active component of silymarin flavonoids that induces apoptosis and in the last 2 decades has been evaluated for the treatment of many tumors (alone or in combination with other chemotherapeutic agents) (Davis-Searles et al., 2005; Kaur et al., 2009). Previously, silibinin was administrated as a supplement in foods for liver diseases remedy (Carrier et al., 2003). Today, the anticancer property of silibinin is known to be related to the presence of flavonoid factors and some strategies to fight cancer cells, including interfering with the cell cycle, inhibiting angiogenesis, invasion, and metastasis through the effect of many molecular events (Denev et al., 2020). This plant extract is an inducer of cancer cell apoptosis and has been investigated for treatment of many tumors (alone or in combination with other chemotherapeutic agents) in the last 2 decades (Ghasemali et al., 2013; Badrzadeh et al., 2014; Jahanafrooz et al., 2018). Nonetheless, hydrophobicity is the most challenging obstacle regarding the application of silibinin in the body (Figure 1) (Iyengar and Devaraj, 2020). Therefore, targeted delivery systems for silibinin are essential to minimize side effects due to systemic drug distribution and achieve a maximum therapeutic effect. This research aimed to study the role of silibinin loaded in MNNPs compared with free drugs in targeting the HT-29 colorectal cancer cell line. To this end, MNNPs and silibinin-loaded MNNPs were synthesized and their physicochemical and morphological properties were evaluated. The MTT assay was done to investigate cell viability. Furthermore, cell cytotoxicity effects, apoptosis, and the cellular uptake rate of MNNPs were examined *in vitro*.

Materials and methods

Materials

Fetal bovine serum (FBS) and trypsin-EDTA were purchased from Gibco (Invitrogen, United Kingdom). Silibinin, DMEM (Dulbecco's Modified Eagle Medium), tween 80, cholesterol, sorbitan monostearate (Span 60), 3-(4,5-dimethylthiazol-2-yl)-2,5-diphenyltetrazolium bromide (MTT), trypsin, dimethyl sulfoxide (DMSO), phosphoric acid, and phosphate-buffered saline (PBS) were obtained from Sigma-Aldrich (St Louis, MO).

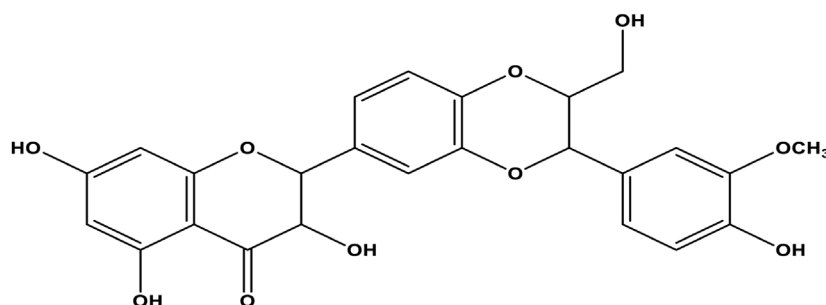


FIGURE 1
Molecular structure of silibinin.

Methanol, chloroform, ethanol, penicillin G, streptomycin, iron (III) chloride, and iron (II) chloride tetrahydrate were purchased from Merck, Germany. Annexin V-FITC apoptosis detection kit [including binding buffer, annexin V, and propidium iodide (PI)] was prepared from eBiosciences (MA, United States).

Cell culture

The HT-29 (colorectal cancer cell line) and HEK-293 (normal cell line) were purchased from the Pasteur Institute cell bank of Iran. The cells were grown in DMEM medium supplemented with FBS (10%), 0.05 mg/mL penicillin G, and 0.08 mg/mL streptomycin. HT-29 colon cancer cells were placed in sterile flasks and incubated at 37°C in a humidified atmosphere containing 5% CO₂.

Synthesis and coating of MNPs

Generally, the co-precipitation method was applied to synthesize MNPs (Kedar et al., 1997). The amount of 6.5 g of FeCl₃ and 4 g of FeCl₂·4H₂O were blended in 100 mL of deionized water in a three-neck flask, and then 200 mL of 2 M NaOH was added dropwise into the flask and stirred for 2 h at a speed rate of 1,000 rpm under N₂ at room temperature. The resulting MNPs were washed twice with distilled water and ethanol (96%) and the final precipitate was placed in a 50°C oven to dry. In the next step, the MNPs were coated with a succinate starch. To synthesize succinate starch, 25 mL of distilled water was added to 4 g of starch, and then 12.5 mL of 2 M NaOH was added to obtain a clear, yellowish solution. Subsequently, 3.7 g of succinic acid (SA) was added to the solution, and the mixture was stirred (1,200 rpm) for 4 h at 100°C. After cooling, 50 mL of cold ethanol (96%) was added to form a white precipitate. Afterward, the sediment was washed several times with ethanol (96%) and dried in an oven at 60°C. To prepare MNPs Ferro fluid, 100 mg of MNPs and 100 mg of succinate starch were mixed in 10 mL of distilled water and stirred (1,000 rpm) for 24 h at room temperature. Finally, the supernatant solution was separated and in order to deposit the iron nanoparticles attached with starch it was placed on a magnet, then the supernatant solution was discarded and the precipitate was collected and dried at room temperature (Fathi et al., 2014; Shahbazi et al., 2023).

Synthesis of NIOs by thin film hydration method

Thin-film hydration method was used to synthesize NIOs. Briefly, 20 mg of Span 60, 15 mg of Tween 80, and 7 mg of cholesterol were dissolved in 6 mL of chloroform and 6 mL of methanol solvents (with a 1:1 ratio). Next, the Solvents were evaporated from the mixture by rotary evaporator (120 rpm, 60°C, 1 h). Finally, a thin layer film of milky surfactant was formed on the wall of the flask. In the next step, 10 mL PBS was added and placed in the rotary for 10 min until the transformation of pro-niosomes to NIOs (Shahbazi et al., 2023). Then, the NIOs suspension was placed in ice bath and exposed to sonication with a probe sonicator (Amplitude of 25%, 200 w) (Fisher Scientific Co., US), to reduce the size of NIOs and to break NIOs aggregates. Silibinin was added in the first step of synthesis due to its lipophilic nature while ferrofluid MNPs were added along with PBS.

MNNPs size, surface charge, and structural characteristics

The dynamic light scattering (DLS) method was used to assess the size and surface charge of synthesized NPs. Furthermore, a transmission electron microscope (TEM) (LEO906E, Carl Zeiss, Oberkochen, Germany), operating at 80 kV was used to determine the size and morphology of the prepared MNNPs. For TEM and FT-IR analysis, the samples were freeze-dried by a freeze-dryer (Dena Vacuum, FD-5005-BT, Iran). Also, Fourier transforms infrared (FT-IR Tensor 27 spectrometer) spectrum (500–4,000 cm⁻¹) was used to evaluate the structural analysis of synthesized NPs, and a vibrating sample magnetometer (VSM) (MDK, Iran) was used to evaluate the magnetization value of MNNPs.

Assessment of drug loading (DL) and encapsulation efficiency (EE) of MNNPs

To determine the amount of loaded silibinin and also to remove the unloaded drug, a dialysis membrane method was performed. Briefly, 5 mL of the silibinin loaded MNNPs were added into a container with 50 mL PBS and magnetically stirred at 120 rpm. To

protect the stability of MNNPs, the container was exposed to the ice. The encapsulation efficiency (EE) and drug loading capacity (DL) were determined by the measurement of unloaded drug via UV-Vis spectroscopy at 288 nm considering the calibration curve by the following formula:

$$EE (\%) = \frac{\text{Mass of drug in NPs}}{\text{Total drug mass}} \times 100$$

$$DL (\%) = \frac{\text{Mass of drug in NPs}}{\text{Total NPs mass}} \times 100$$

Assessment of drug release rate of MNNPs

First, the MNNPs containing silibinin were transferred to two clamped dialysis bags that were inserted in distilled water for 24 h. For the simulation of normal and abnormal (cancer) conditions, PBS (pH = 7.4) and composed of methanol and 0.02 M phosphoric acid (50: 50, v/v) (pH = 5.8) were used, respectively. Buffer solutions (50 mL of each) were added into two lidded containers, and the dialysis bags were exposed to buffers. Bags were shaken (100 rpm) at 37°C. At different time intervals, 2 mL of the sample was replaced with 2 mL of fresh solution. The release pattern was calculated using UV-Vis spectrophotometer at 288 nm. Also, the release curves were evaluated by various kinetic models (Fathi et al., 2018).

MTT assay

The cytotoxicity of drugs was evaluated by MTT assay, briefly, 6.5×10^3 HT-29 and HEK-293 cells/well were seeded in a 96-well plate and incubator at 37°C with 5% CO₂ for 24 h. Afterward, cells were exposed to various doses of free and encapsulated silibinin and incubated for 24 and 48 h. After the required incubation time, 50 µL of the MTT solution (2 mg/mL) was added to each well, and plates were covered with an aluminum foil and incubated for 4 h. After this time, the supernatant was removed, and 100 µL of DMSO was added and shaken for 10 min. Finally, the plates were transferred to the ELISA reader (Biotech Co., United States), and the optical densities (ODs) were read at a reference wavelength of 570 nm in comparison to untreated control cells.

Cell apoptosis assessment

Flow cytometry technique was used to analyze cell apoptosis, in summary, 70,000 HT-29 cells were seeded to each well in 6-well plates. For cell treatment, silibinin and NIOs complex (40 µg/mL) were used and treated for 48 h. After separating, the cells were washed twice with PBS and centrifuged at 190 g for 5 min. Then, 100 µL of binding buffer, 5 µL of FITC (0.25 µg/mL), and 5 µL of propidium iodide (20 µg/mL) were added to each sample and left for 20 min in the dark at room temperature. Finally, 100 µL of binding buffer (0.1 M Hepes (pH 7.4), 1.4 M NaCl, and 25 mM CaCl₂) was added, and reading was performed using a flow cytometry device (Thermo Fisher Scientific Co., United States) in the darkness.

Assessment of cellular uptake of NIOs

For this purpose, 5 mg of FITC was dissolved in 1 mL of methanol, and 250 µL was added to each falcon and mixed with 1 mL of niosomal complexes. Covered falcons were placed in a shaker with ice at a speed of 100 rpm overnight, and then the contents of the falcons were washed in two steps under dark conditions using PBS. Subsequently, 70,000 HT-29 cells were seeded in each well of 6-well plates and exposed to niosomal complex for 4 h in the darkness in a humidified atmosphere containing 5% CO₂. After the treatment, the cells were transferred to falcons and centrifuged for 5 min at 190 g, after discarding the supernatant, washed with PBS and centrifuged, and this process was repeated and finally, the reading was done with a flow cytometry device.

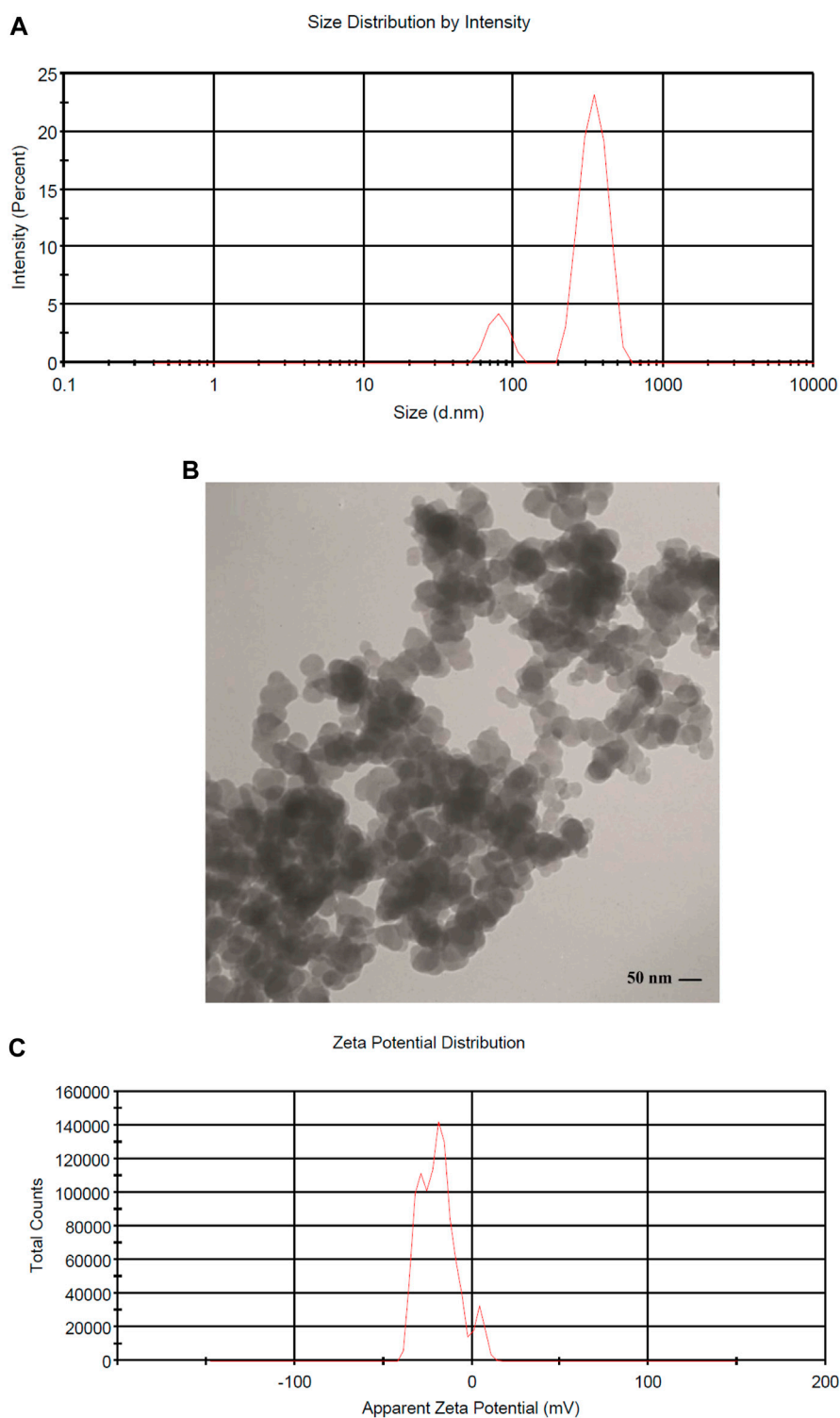
Statistical analysis

Statistical analysis was performed using the non-parametric paired Wilcoxon test and statistical significance was described when the *p*-value was less than 0.05. All statistical analyzes were performed by Flowjo-V10 and Prism software version 9.3. The results were expressed as the mean ± standard deviation (SD) of three independent experiments.

Results and discussion

Measurement and characterization of synthesized MNNPs

Generally, MNNPs size is one of the principal characteristics regarding the release of the drug from the MNNPs, physical stability, cellular absorption, and biological distribution (Barani et al., 2019). The size and surface charge of the synthesized MNNPs were checked using the DLS method. The distribution intensity of MNNPs was obtained at 70 nm with DLS (Figure 2A). According to the TEM image, shapes and distributions of MNNPs were homogeneous spherical with a size of 50 nm (Figure 2B). Typically, the size of MNNPs in the TEM images was smaller than in DLS as DLS, the hydrodynamic diameter of the MNNPs was measured. The larger MNNPs in the images are associated with the overlapping/agglomeration of some smaller MNNPs during the preparation (Liu et al., 2021). Lately, researchers have focused on the surfactants coating the MNNPs, because they can act as a steric barrier and intercept agglomeration caused by magnetic dipole-dipole attractions between MNNPs (Ramimoghadam et al., 2015). The different sizes have been reported by previous research, and it seems that other physical attributes of MNNPs like surface charge as well as different structures of chemical compounds and synthesis methods are responsible for the size of MNNPs (Barani et al., 2020; Ag Seleci et al., 2021). Considering that NPs in the range of 70–200 nm are stable in the bloodstream and are considered long-circulating agents, synthesized MNNPs with the above size can be used for smart drug delivery in pharmaceutical purposes, according to previous published studies (Barar and Omid, 2014).

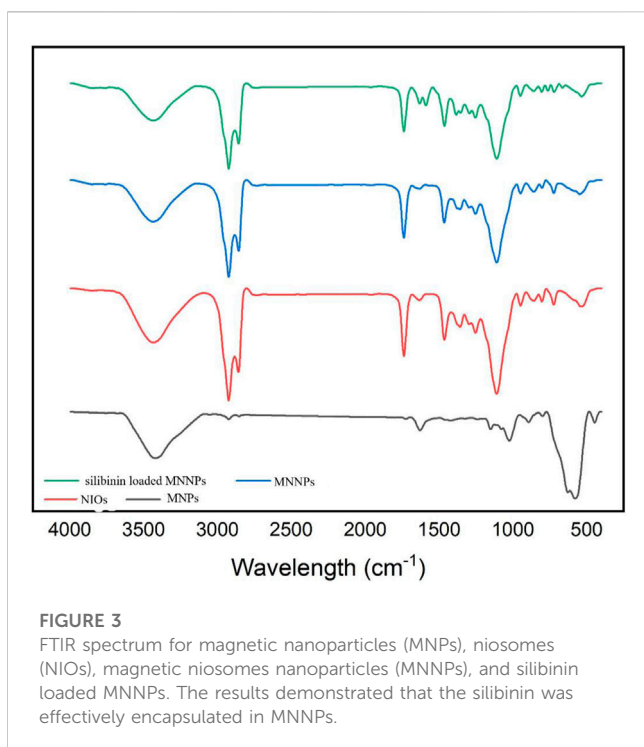
**FIGURE 2**

(A) DLS histogram showing the size distribution intensity of magnetic niosome NPs MNNPs, (B) Characterization of MNNPs size and morphology using Transmission Electron Microscopy (TEM), and (C) zeta potential distribution of MNNPs.

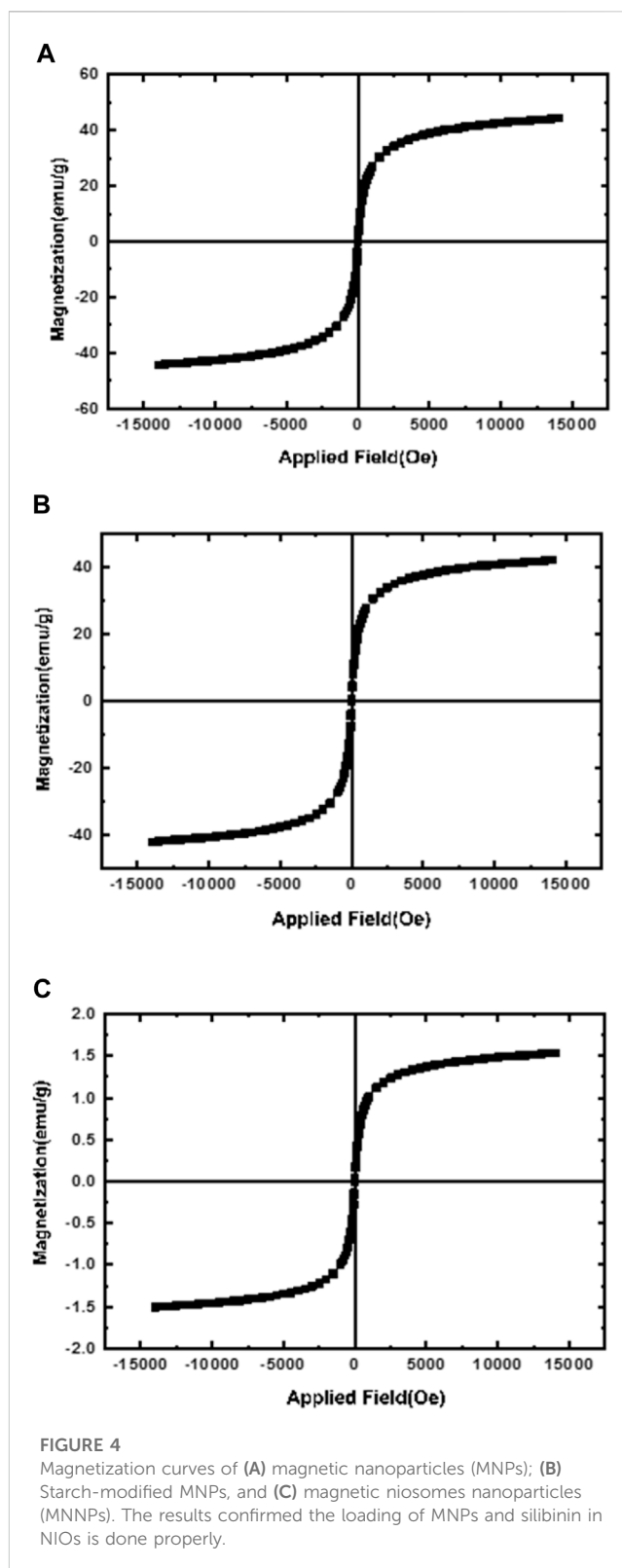
In addition, it was demonstrated that NPs less than 200 nm can be escaped of the immunes system, while NPs with size less than 70 nm can be accumulated by the liver (Barar and Omid, 2014). MNNPs charge is another important feature that has a

considerable impact in entering and capturing the drug into the cell and size distribution of MNNPs.

It is established that making a targeted surface charge of synthesized NPs is a practical strategy to control their



assimilation into the particular destination (Osaka et al., 2009; Stiufluic et al., 2013). Usually, a positive charge of NPs surface through coating leads to convenient and fast cellular uptake when NPs are encountered with the negative charge on the cell membrane (Su et al., 2012). In this research, the surface charge of the synthesized MNNPs was determined using the DLS method as the zeta potential was -19.0 mV (Figure 2C) and polydispersity index (PDI) was 0.52. The zeta potential result reveals that the surface charges of synthesized MNNPs are negative. This negative charge reduces the toxicity of the system and improves its performance by preventing the accumulation and deposition of NPs. FT-IR technique was used to study the chemical structure of the prepared MNNPs, and to measure the non-interaction of the synthesized niosomal system with silibinin and MNPs. Expected peaks related to MNPs, modified NIOs, MNNPs, and silibinin loaded MNNPs were monitored, which indicated that silibinin and MNPs were loaded in NIOs (Figure 3). In examining the FT-IR spectrum of drug-free NIOs (Figure 3), the peak at $3,433$ cm^{-1} is characteristic of the -OH group and the peak at $1,738$ cm^{-1} is related to C=O stretching vibrations. Finally, the peaks at $2,923$ cm^{-1} and $1,109$ cm^{-1} are related to the C-H bond and vibrations of C-O bond stretching, respectively (Mehta and Jindal, 2013; Samed et al., 2018). For NIOs containing silibinin and MNPs, the peak at $1,631$ cm^{-1} corresponds to C=O stretching vibrations, and the peak at $3,435$ cm^{-1} is associated with the -CH bond. Furthermore, the absorption peaks at $2,923$ cm^{-1} , $1,108$ cm^{-1} , and 720 cm^{-1} belong to the C-H bond, stretching vibrations of the C-O bond, and Fe-O bond in Fe_3O_4 , respectively (Ebrahimnezhad et al., 2013). By comparing the peaks in the FT-IR spectrum related to NIOs, MNNPs, and silibinin loaded MNNPs, it was observed that slight changes occurred in the peaks related to NIOs containing silibinin compared to NIOs without drug, and this confirmed that



silibinin drug is placed in the NIOs niosome. Also, considering that no new peak was added and disappeared in the FT-IR spectrum of NIOs containing the drug, it can be assumed that no chemical interaction occurred between the NIOs and the drug as both kept their nature and remained away from change.

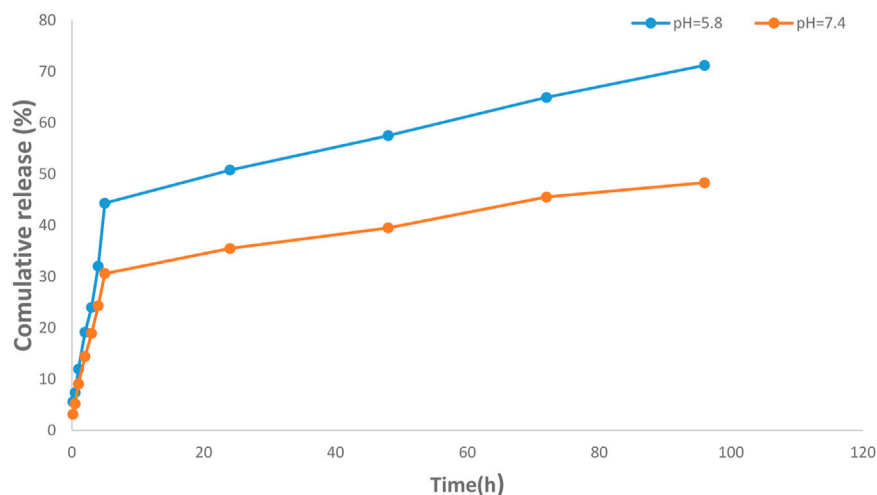


FIGURE 5

Investigation of drug release efficiency from magnetic nisome nanoparticles (MNNPs) at pH = 5.8 and 7.4 at 37°C. The pores of the dialysis membrane are large enough to allow the free movement of silibinin, but small enough to prevent the diffusion of nanoparticles. The results demonstrated a sustained release pattern from the nanoparticle with a partially burst-release at the initial stage and followed sustained during the 96 h study period. Data are presented as mean \pm SD of three independent experiments.

Vibrating sample magnetometer (VSM) was used to evaluate the superparamagnetism of NPs. Since the reason for using magnetic NPs is the targeted delivery of the carrier by applying an external magnetic field, it is very important and necessary to determine the magnetic properties of these NPs. The magnetic activities of MNNPs, starch modified MNPs, and MNPs were demonstrated using vibrating sample magnetometry (VSM) at room temperature. The hysteresis curve in Figure 4A; Figure 4B showed that the saturation magnetization of MNPs was 42 emu/g. Compared to the saturation magnetization of MNNPs in Figure 4C, which is 1.5 emu/g, this value is higher. This difference confirms that the loading of MNPs and silibinin in NIOs is done properly, according to previous studies published in this area. The Figure 4 does not show any hysteresis curve indicating the superparamagnetic behavior of the synthesized particles (Yang et al., 2006).

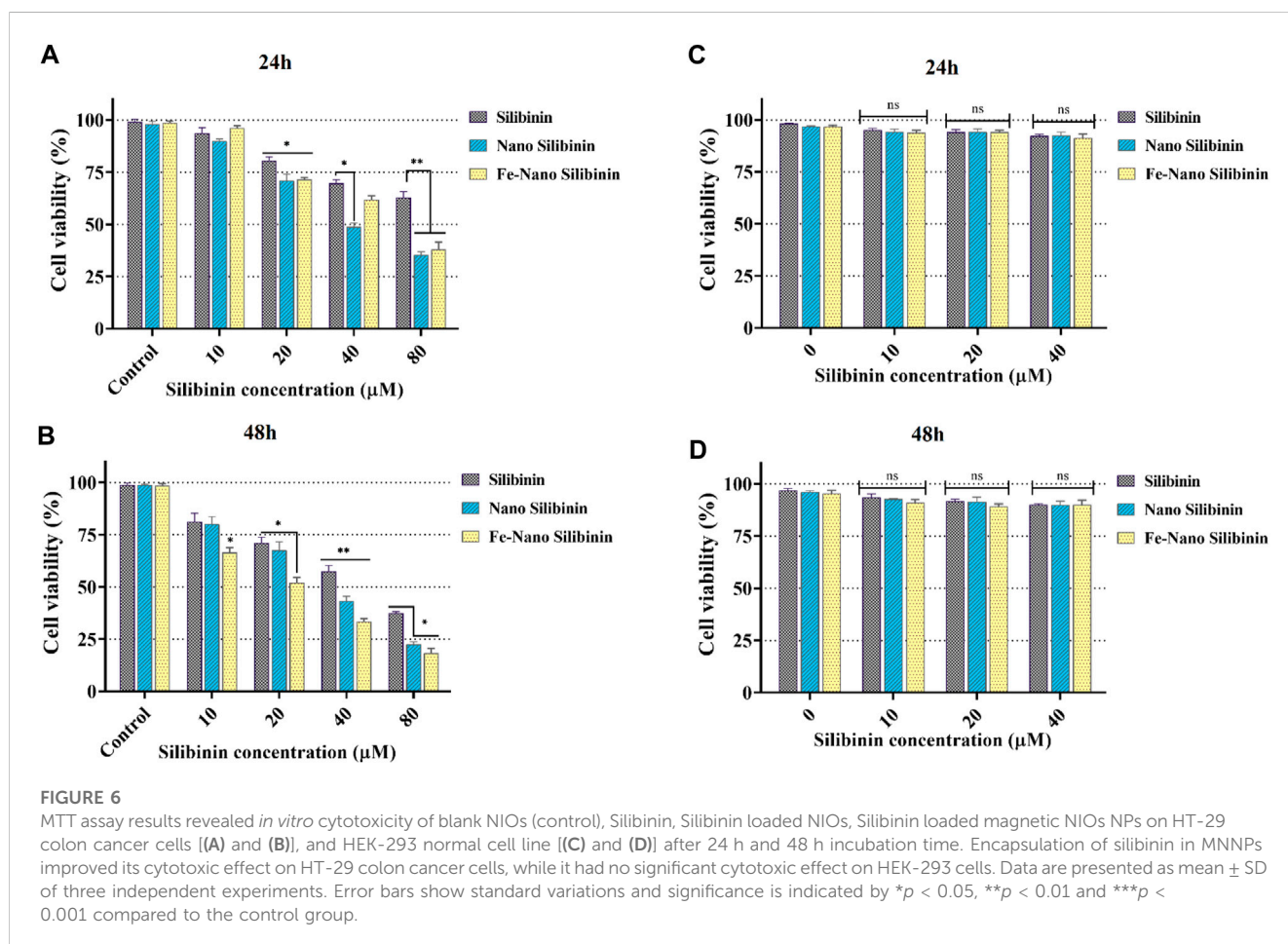
Encapsulation efficiency, drug release rate of MNNPs and kinetics models

Encapsulation efficiency (EE) is defined as the ratio of the amount of drug in the MNNPs to the total amount of drug applied in NPs formulation. Currently, a large number of NPs systems have relatively low EE, thus developing strategies to increase EE remains a challenge (Liu et al., 2019). EE has been increased while there is a drug concentration increase thanks to polymers and MNNPs, based on the previously published studies (Prabha and Raj, 2016; Ghadiri et al., 2017; Erdagi and Yildiz, 2019). Jin et al. (2018) argued lowering the pH is a promising way to boost the EE efficiency up to approximately 70% in the MNNPs formation while this efficiency without pH change is between 10% and 15% at maximum. In the present study, the EE in NIOs was more than 90%, which

indicates the high potential of MNNPs in EE. Span 60 and also cholesterol which are used in the NIOs structure increase the amount of the hydrophobic drug loading into NIOs (Jadon et al., 2009). The results indicated the release of the silibinin with a gentle and slow gradient from MNNPs. Evaluating the drug release pattern shows that the designed NIOs, while indicating a controlled release, have a burst release within 4 h, then in the conditions of normal cells (pH 7.4) and cancer cells (pH 5.8) released about 49% and 70%, respectively during 100 h (Figure 5). These findings reveal that MNNPs are sensitive to different pH. The high acidity of tumor cells is attributed to hypoxia, or lack of oxygen owing to the inadequate blood supply (Justus et al., 2013). It was demonstrated that the MNNPs indicated better performance in tumor microenvironment (pH 5.0–6.8) compared to the physiological condition which make them the suitable candidate for DDS (Mohammadian et al., 2016b; Myat et al., 2022). Considering that tumor cells have a significantly acidic cytoplasmic pHs compared to normal cells, therefore MNNPs are more efficient with more DR at acidic pH compared to pH = 7.4 (AlSawafthah et al., 2022). This makes NIOs a good candidate for drug delivery in cancer. The results indicated the release of the silibinin with a gentle and slow gradient from MNNPs. Our findings are in agreement with previous studies that confirmed the promising role of MNNPs in the drug release process. Barani et al. reported, the drug's release profile from MNNPs showed a first rapid release (about 50% of the drug was released within 10 h), followed by a slower and longer-lasting release (65% of the drug was released within 30 h) in acidic conditions (Barani et al., 2019). Similar outcomes were obtained by Zheng et al. (2009) Preparation and definition of magnetic cationic liposomes for gene transfer research. Tavano et al. (2013) synthesized MNNPs loading doxorubicin (an anticancer drug) for smart drug delivery and argued that the utilization

TABLE 1 The kinetics models used to fit the silibinin release data from MNNPs at different pHs. The bold values indicated the best fitted models.

Kinetics model	Equation	Coefficient of determination (R^2)	
		pH = 5.8	pH = 7.4
Zero order	$F = k_0 t$	0.7542	0.7274
First order	$\ln(1 - F) = -k_f t$	0.8673	0.7959
Higuchi	$F = k_H \sqrt{t}$	0.9030	0.8896
Power law	$\ln F = \ln k_p + P \ln t$	0.9506	0.9627
Square root of mass	$1 - \sqrt{1 - F} = k_{1/2} t$	0.8131	0.7622
Hixson-Crowell	$1 - \sqrt[3]{1 - F} = k_{1/3} t$	0.8319	0.7736
Three seconds' root of mass	$1 - \sqrt[3]{(1 - F)^2} = k_{2/3} t$	0.7937	0.7507
Weibull	$\ln(-\ln(1 - F)) = -\beta \ln t_d + \beta \ln t$	0.9462	0.9208
Reciprocal powered time	$(\frac{1}{F} - 1) = \frac{m}{t^b}$	0.9610	0.9365



of MNNPs can improve the release rate of formulations. Table 1 shows various kinetic models that were used to fit the silibinin release curves at different pHs. According to Table 1, the fitted model for release curves were Power law and Reciprocal powered time at pH = 7.4 and 5.8.

Cell cytotoxicity of MNNPs

Through receptor-mediated endocytosis, targeted NPs can enter the target cells, increasing the concentration of drug molecules within the cell. P-glycoprotein does not recognize drug molecules

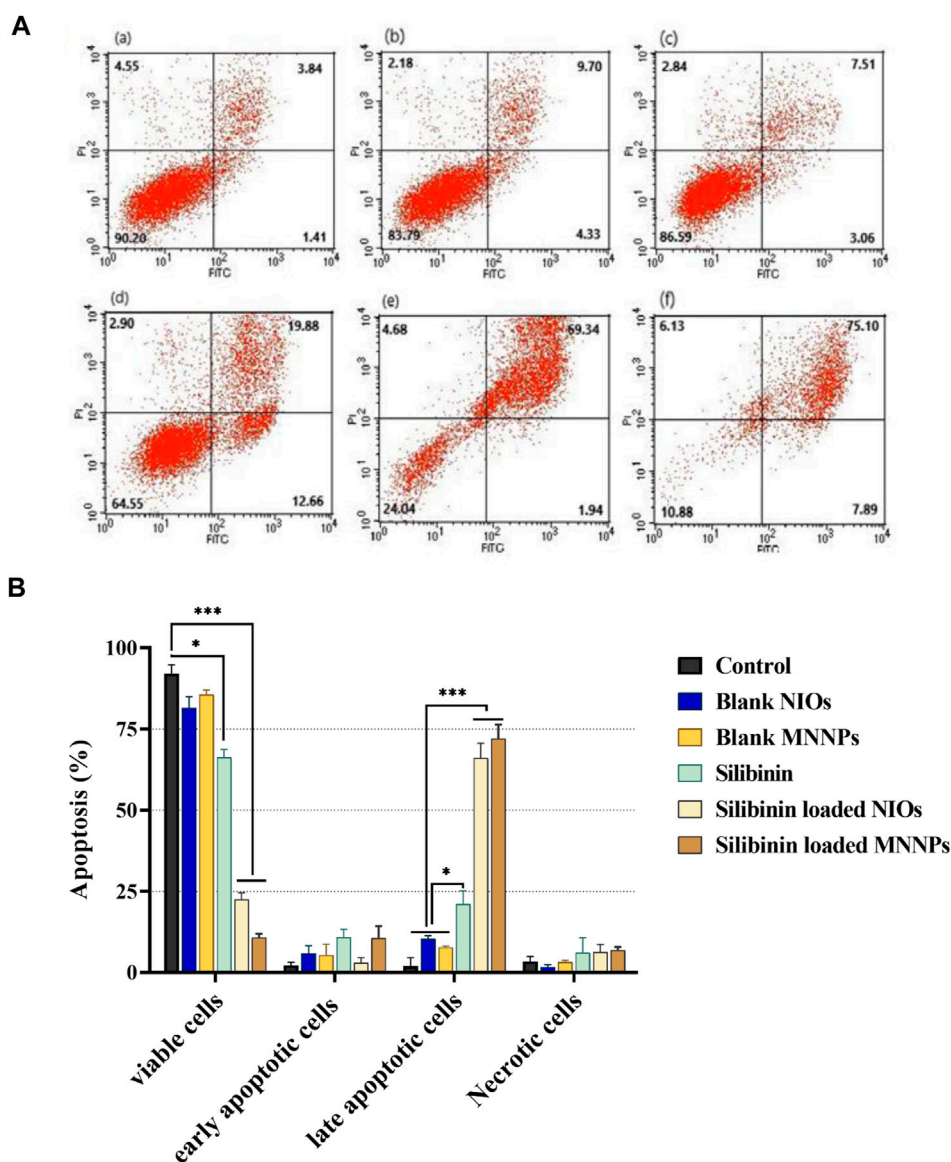


FIGURE 7

(A). Apoptosis analysis on HT-29 cell line under treatment (a) control, (b) blank NIOs, (c) blank MNNPs, (d) Silibinin, (e) Silibinin loaded NIOs, (f) Silibinin loaded MNNPs. (B). HT-29 cells treated with pure silibinin and niosomal complexes were evaluated after 48 h by FITC-labeled annexin V/PI flow cytometry. The obtained results confirmed that NIOs loaded with the silibinin significantly increase the apoptosis of HT-29 cells, which emphasizes the increase in the absorption of drugs from NIOs by the cells. This result is consistent with the MTT results. Data were analyzed using Flowjo-V10 analysis software and shown as mean ± SD of three independent experiments. Significance is indicated by * $p < 0.05$, ** $p < 0.01$ and *** $p < 0.001$ compared to the control group.

during this process, and membrane efflux transporters pump free drug molecules out of the cell (Wang et al., 2016). In the cell cytotoxicity assessment by the MTT method, HT-29 and HEK-293 cells were treated with free-drug and silibinin MNNPs for 24 and 48 h at various concentrations (10, 20, 40, and 80 µg/mL) (Figure 6). The results showed that NIOs containing silibinin caused more cell death in the studied times compared to pure silibinin in the HT-29 colon cancer cells and had no significant cytotoxic effect on HEK-293 cells. Thus, nanocarriers can increase the cell cytotoxicity of the drug against HT-29 cells, and there is a dose-dependent and relatively time-dependent manner regarding using complex. These

results confirm the previous studies reported that the cytotoxicity of the drug-loaded MNNPs follows dose-dependent and time-dependent trends (Huang et al., 2015; Dhavale et al., 2021). The IC50 of the MNNPs complex was observed at 40 µg/mL within 48 h, therefore this concentration was considered for the following tests. The survival of over 90% of cells under drug-free NIOs treatment revealed that MNNPs have a very tiny lethal effect on the cells. This biocompatibility makes these MNNPs excellent candidates for therapeutic purposes. Additionally, the MTT test revealed that there was no significant correlation between the control group and silibinin-free NIOs.

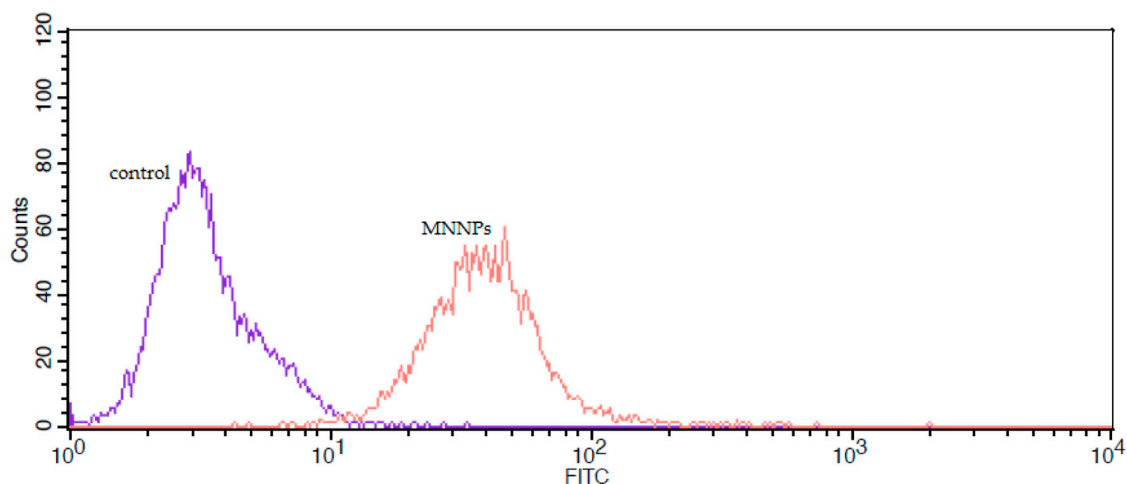


FIGURE 8

The flow cytometry analysis of uptake of FITC-labeled magnetic niosome nanoparticles (MNNPs) by HT-29 cells.

Apoptosis and cellular uptake analysis on HT-29 cell line

HT-29 cells that treated with pure silibinin and silibinin loaded MNNPs were evaluated after 48 h incubation by FITC-labeled Annexin V/PI flow cytometry technique. As shown in Figure 7, silibinin-loaded MNNPs significantly induce apoptosis of HT-29 cells more than other forms, furthermore, silibinin-loaded MNNPs exhibited a greater cytotoxic effect compared to the free silibinin, which demonstrates the increase in the uptake of silibinin from MNNPs by the cells. These findings are consistent with earlier research, which indicated that the internalization and subsequent intracellular release of the anticancer drug from NPs is responsible for the cytotoxic effect of NPs (Zaki, 2014). It is proposed that this formulation (niosome and magnetic niosome) can increase the drug bioavailability which can induce cancer cell apoptosis by causing DNA damage or the oxidation of proteins, lipids, and enzymes, resulting in cell death and also helping to destroy and inhibit the mitochondrial respiratory complex (Rodrigues Pereira da Silva et al., 2016; Van Houten et al., 2016; Juan et al., 2021). El-Far and co. argued that the cytotoxicity percentage by IC50 value between paclitaxel-metal NPs-NIOs and oxaliplatin-metal NPs-NIOs at the same concentrations did not differ significantly (pH 0.5). Therefore, they recommended that MNNPs are considered a suitable targeting nanocarrier system for drug delivery in colorectal cancer, target tumor cells and prolong circulation for both drugs (El-Far et al., 2022).

Also, cellular uptake was studied by FITC labeled NPs and via flow cytometry. Figure 8 illustrates the cellular uptake level of MNNPs by the HT-29 cell line was 99% compared to the control group. These findings indicated that the MNNPs could enhance cellular uptake significantly and induce apoptosis in the HT-29 cell line after treatment, and are consistent with previous studies that used flow cytometry to examine apoptosis and MNP uptake in cells (Depan and Misra, 2012; Li et al., 2018; Lu et al., 2018).

Conclusion

In the current study, silibinin was loaded into NIOs containing MNPs (MNNPs) as a novel formulation to evaluate its apoptosis effect in colorectal cancer cells treatment. The size distribution, surface charge, and chemical structure of synthesized MNNPs were suitable for immune escape and confirmed that silibinin was entrapped in NIOs. According to the obtained cytotoxicity evaluations, silibinin loaded in MNNPs has more cytotoxic effects on HT-29 colon cancer cells in a dose- and time-dependent manner, and the cellular uptake of MNNPs by the HT-29 cell line was higher than controls. Drug loading evaluation exhibited a high efficiency and drug-loaded MNNPs showed an accelerated release rate in acidic pH in cancer cells compared to the neutral condition. To sum up, the MNNPs as nanocarriers are excellent candidates for the treatment of cancer cells, especially colorectal cancer. However, further *in vivo* experiments are required to prove the potential of the developed formulation as a suitable vehicle for the various cancerous cells treatment.

Data availability statement

The original contributions presented in the study are included in the article/supplementary materials, further inquiries can be directed to the corresponding author.

Author contributions

GS: Methodology, Investigation, Data curation, Original draft preparation. DJ and MF: Methodology, Investigation, Data curation, Original draft preparation. MF: Methodology, Investigation, Original draft preparation. EA: Reviewing and Editing. NZ: Supervision, Conceptualization, Writing- Reviewing and Editing. All authors contributed to the article and approved the submitted version.

Funding

This study is a part of an MSc thesis (Grant no: 68129) and the authors acknowledge the financial support provided by the Research Vice-Chancellor of Tabriz University of Medical Sciences.

Acknowledgments

The authors want to thank the Research Center for Pharmaceutical Nanotechnology and Department of Medical Biotechnology, Faculty of Advanced Medical Sciences at Tabriz University of Medical Sciences for technical supports.

References

- Ag Seleci, D., Maurer, V., Barlas, F. B., Porsiel, J. C., Temel, B., Ceylan, E., et al. (2021). Transferrin-decorated niosomes with integrated InP/ZnS quantum dots and magnetic iron oxide nanoparticles: Dual targeting and imaging of glioma. *Int. J. Mol. Sci.* 22 (9), 4556. doi:10.3390/ijms22094556
- Alagheband, Y., Jafari-gharabaghlu, D., Imani, M., Mousazadeh, H., Dadashpour, M., Firouzi-Amandi, A., et al. (2022). Design and fabrication of a dual-drug loaded nano-platform for synergistic anticancer and cytotoxicity effects on the expression of leptin in lung cancer treatment. *J. Drug Deliv. Sci. Technol.* 73, 103389. doi:10.1016/j.jddst.2022.103389
- AlSawafah, N. M., Awad, N. S., Pitt, W. G., and Husseini, G. A. (2022). pH-responsive nanocarriers in cancer therapy. *Polymers* 14 (5), 936. doi:10.3390/polym14050936
- Badrzadeh, F., Akbarzadeh, A., Zarghami, N., Yamchi, M. R., Zeighamian, V., Tabatabae, F. S., et al. (2014). Comparison between effects of free curcumin and curcumin loaded NIPAAm-MAA nanoparticles on telomerase and PinX1 gene expression in lung cancer cells. *Asian Pac. J. Cancer Prev.* 15 (20), 8931–8936. doi:10.7314/apjcp.2014.15.20.8931
- Barani, M., Nematollahi, M. H., Zaboli, M., Mirzaei, M., Torkzadeh-Mahani, M., Pardakhty, A., et al. (2019). *In silico* and *in vitro* study of magnetic niosomes for gene delivery: The effect of ergosterol and cholesterol. *Mater. Sci. Eng. C* 94, 234–246. doi:10.1016/j.msec.2018.09.026
- Barani, M., Torkzadeh-Mahani, M., Mirzaei, M., and Nematollahi, M. H. (2020). Comprehensive evaluation of gene expression in negative and positive trigger-based targeting niosomes in HEK-293 cell line. *Iran. J. Pharm. Res. IJPR.* 19 (1), 166–180. doi:10.22037/ijpr.2019.112058.13507
- Barar, J., and Omid, Y. (2014). Surface modified multifunctional nanomedicines for simultaneous imaging and therapy of cancer. *BiolImpacts BI* 4 (1), 3–14. doi:10.5681/bi.2014.011
- Bray, F., Ferlay, J., Soerjomataram, I., Siegel, R. L., Torre, L. A., and Jemal, A. (2018). Global cancer statistics 2018: GLOBOCAN estimates of incidence and mortality worldwide for 36 cancers in 185 countries. *CA a cancer J. Clin.* 68 (6), 394–424. doi:10.3322/caac.21492
- Carrier, D. J., Crowe, T., Sokhansanj, S., Wahab, J., and Barl, B. (2003). Milk thistle, *Silybum marianum* (L) Gaertn, flower head development and associated marker compound profile. *J. herbs, spices Med. plants* 10 (1), 65–74. doi:10.1300/j044v10n01_08
- Coviello, T., Trotta, A., Marianecci, C., Carafa, M., Di Marzio, L., Rinaldi, F., et al. (2015). Gel-embedded niosomes: Preparation, characterization and release studies of a new system for topical drug delivery. *Colloids surfaces B biointerfaces* 125, 291–299. doi:10.1016/j.colsurfb.2014.10.060
- Davis-Searles, P. R., Nakanishi, Y., Kim, N. C., Graf, T. N., Oberlies, N. H., Wani, M. C., et al. (2005). Milk thistle and prostate cancer: Differential effects of pure flavonolignans from *Silybum marianum* on antiproliferative end points in human prostate carcinoma cells. *Cancer Res.* 65 (10), 4448–4457. doi:10.1158/0008-5472.CAN-04-4662
- Denev, P., Ognyanov, M., Georgiev, Y., Teneva, D., Klisurova, D., and Yanakieva, I. Z. (2020). Chemical composition and antioxidant activity of partially defatted milk thistle (*Silybum marianum* L) seeds. *Bulg. Chem. Commun.* 52, 182–187.
- Depan, D., and Misra, R. (2012). Hybrid nanoparticle architecture for cellular uptake and bioimaging: Direct crystallization of a polymer immobilized with magnetic nanoparticles on carbon nanotubes. *Nanoscale* 4 (20), 6325–6335. doi:10.1039/c2nr31345f
- Dhvale, R. P., Dhavale, R., Sahoo, S., Kollu, P., Jadhav, S., Patil, P., et al. (2021). Chitosan coated magnetic nanoparticles as carriers of anticancer drug telmisartan: pH-responsive controlled drug release and cytotoxicity studies. *J. Phys. Chem. Solids* 148, 109749. doi:10.1016/j.jpcs.2020.109749

Conflict of interest

The authors declare that the research was conducted in the absence of any commercial or financial relationships that could be construed as a potential conflict of interest.

Publisher's note

All claims expressed in this article are solely those of the authors and do not necessarily represent those of their affiliated organizations, or those of the publisher, the editors and the reviewers. Any product that may be evaluated in this article, or claim that may be made by its manufacturer, is not guaranteed or endorsed by the publisher.

Eatemadi, A., Daraee, H., Aiyelabegan, H. T., Negahdari, B., Rajeian, B., and Zarghami, N. (2016). Synthesis and characterization of chrysin-loaded PCL-PEG-PCL nanoparticle and its effect on breast cancer cell line. *Biomed. Pharmacother.* 84, 1915–1922. doi:10.1016/j.biopha.2016.10.095

Ebrahimzadeh, Z., Zarghami, N., Keyhani, M., Amirasaad, S., Akbarzadeh, A., Rahmati, M., et al. (2013). Inhibition of hTERT gene expression by silibinin-loaded PLGA-PEG-Fe₃O₄ in T47D breast cancer cell line. *BiolImpacts BI* 3 (2), 67–74. doi:10.5681/bi.2013.005

El-Far, S. W., Abo El-Enin, H. A., Abdou, E. M., Nafea, O. E., and Abdelmonem, R. (2022). Targeting colorectal cancer cells with niosomes systems loaded with two anticancer drugs models; comparative *in vitro* and anticancer studies. *Pharmaceuticals* 15 (7), 816. doi:10.3390/ph15070816

Erdagi, S. I., and Yildiz, U. (2019). Diosgenin-conjugated PCL-MPEG polymeric nanoparticles for the co-delivery of anticancer drugs: Design, optimization, *in vitro* drug release and evaluation of anticancer activity. *New J. Chem.* 43 (17), 6622–6635. doi:10.1039/c9nj00659a

Fathi, M., Entezami, A. A. J. S., and Analysis, I. (2014). Stable aqueous dispersion of magnetic iron oxide core-shell nanoparticles prepared by biocompatible maleate polymers. *Surf. Interface Anal.* 46 (3), 145–151. doi:10.1002/sia.5362

Fathi, M., Zangabad, P. S., Barar, J., Aghanejad, A., Erfan-Niya, H., and Yjijobm, O. (2018). Thermo-sensitive chitosan copolymer-gold hybrid nanoparticles as a nanocarrier for delivery of erlotinib. *Int. J. Biol. Macromol.* 106, 266–276. doi:10.1016/j.ijbiomac.2017.08.020

Ghadiri, M., Vasheghani-Farahani, E., Atyabi, F., Kobarfard, F., Mohamadyar-Toupanlou, F., and Hosseinkhani, H. (2017). Transferrin-conjugated magnetic dextran-spermine nanoparticles for targeted drug transport across blood-brain barrier. *J. Biomed. Mater. Res. Part A* 105 (10), 2851–2864. doi:10.1002/jbm.a.36145

Ghasemali, S., Nejati-Koshki, K., Akbarzadeh, A., Tafsiri, E., Zarghami, N., Rahmati-Yamchi, M., et al. (2013). Inhibitory effects of β -cyclodextrin-helenalin complexes on H-TERT gene expression in the T47D breast cancer cell line-results of real time quantitative PCR. *Asian Pac. J. Cancer Prev.* 14 (11), 6949–6953. doi:10.7314/apjcp.2013.14.11.6949

Hassani, N., Jafari-Gharabaghlu, D., Dadashpour, M., and Zarghami, N. (2022). The effect of dual bioactive compounds artemisinin and metformin co-loaded in PLGA-PEG nanoparticles on breast cancer cell lines: Potential apoptotic and anti-proliferative action. *Appl. Biochem. Biotechnol.* 194 (10), 4930–4945. doi:10.1007/s12010-022-04000-9

Huang, Y., Zhou, Z., Liang, J., Ding, P., Cao, L., Chen, Z., et al. (2015). Preparation, characterisation and *in vitro* cytotoxicity studies of chelerythrine-loaded magnetic Fe₃O₄@ O-carboxymethylchitosan nanoparticles. *J. Exp. Nanosci.* 10 (7), 483–498. doi:10.1080/17458080.2013.843209

Hulvat, M. C. (2020). Cancer incidence and trends. *Surg. Clin.* 100 (3), 469–481. doi:10.1016/j.suc.2020.01.002

Iyengar, R. M., and Devaraj, E. (2020). Silibinin triggers the mitochondrial pathway of apoptosis in human Oral squamous carcinoma cells. *Asian Pac. J. Cancer Prev. APJCP.* 21 (7), 1877–1882. doi:10.31557/APJCP.2020.21.7.1877

Jadid, M. F. S., Jafari-Gharabaghlu, D., Bahrami, M. K., Bonabi, E., and Zarghami, N. (2023). Enhanced anti-cancer effect of curcumin loaded-niosomal nanoparticles in combination with heat-killed *Saccharomyces cerevisiae* against human colon cancer cells. *J. Drug Deliv. Sci. Technol.* 80, 104167. doi:10.1016/j.jddst.2023.104167

Jadon, P. S., Gajbhiye, V., Jadon, R. S., Gajbhiye, K. R., and Ganesh, N. (2009). Enhanced oral bioavailability of griseofulvin via niosomes. *AAPS pharmscitech* 10, 1186–1192. doi:10.1208/s12249-009-9325-z

Jafari-Gharabaghlu, D., Dadashpour, M., Khanghah, O. J., Salmani-Javan, E., and Zarghami, N. (2023). Potentiation of folate-functionalized PLGA-PEG nanoparticles

- loaded with metformin for the treatment of breast cancer: Possible clinical application. *Mol. Biol. Rep.* 50, 3023–3033. doi:10.1007/s11033-022-08171-w
- Jahanafrooz, Z., Motamed, N., Rinner, B., Mokhtarzadeh, A., and Baradaran, B. (2018). Silibinin to improve cancer therapeutic, as an apoptotic inducer, autophagy modulator, cell cycle inhibitor, and microRNAs regulator. *Life Sci.* 213, 236–247. doi:10.1016/j.lfs.2018.10.009
- Jamshidifar, E., Eshtrati Yeganeh, F., Shayan, M., Tavakkoli Yarak, M., Bourbour, M., Moammeri, A., et al. (2021). Super magnetic niosomal nanocarrier as a new approach for treatment of breast cancer: A case study on SK-BR-3 and MDA-MB-231 cell lines. *Int. J. Mol. Sci.* 22 (15), 7948. doi:10.3390/ijms22157948
- Jin, M., Jin, G., Kang, L., Chen, L., Gao, Z., and Huang, W. (2018). Smart polymeric nanoparticles with pH-responsive and PEG-detachable properties for co-delivering paclitaxel and survivin siRNA to enhance antitumor outcomes. *Int. J. Nanomedicine* 13, 2405–2426. doi:10.2147/IJN.S161426
- Juan, C. A., Pérez de la Lastra, J. M., Plou, F. J., and Pérez-Lebeña, E. (2021). The chemistry of reactive oxygen species (ROS) revisited: Outlining their role in biological macromolecules (DNA, lipids and proteins) and induced pathologies. *Int. J. Mol. Sci.* 22 (9), 4642. doi:10.3390/ijms22094642
- Justus, C. R., Dong, L., and Yang, L. V. (2013). Acidic tumor microenvironment and pH-sensing G protein-coupled receptors. *Front. Physiology* 4, 354. doi:10.3389/fphys.2013.00354
- Kaur, M., Velmurugan, B., Tyagi, A., Deep, G., Katiyar, S., Agarwal, C., et al. (2009). Silibinin suppresses growth and induces apoptotic death of human colorectal carcinoma LoVo cells in culture and tumor xenograft. *Mol. Cancer Ther.* 8 (8), 2366–2374. doi:10.1158/1535-7163.MCT-09-0304
- Kedar, E., Palgi, O., Golod, G., Babai, I., and Barenholz, Y. (1997). Delivery of cytokines by liposomes. III. Liposome-encapsulated GM-CSF and TNF-alpha show improved pharmacokinetics and biological activity and reduced toxicity in mice. *J. Immunother.* 20 (3), 180–193. doi:10.1097/00002371-199705000-00003
- Li, J., Wang, X., Zheng, D., Lin, X., Wei, Z., Zhang, D., et al. (2018). Cancer cell membrane-coated magnetic nanoparticles for MR/NIR fluorescence dual-modal imaging and photodynamic therapy. *Biomaterials Sci.* 6 (7), 1834–1845. doi:10.1039/c8bm00343b
- Liu, F., Jin, H., Wang, Y., Chen, C., Li, M., Mao, S., et al. (2017). Anti-CD123 antibody-modified niosomes for targeted delivery of daunorubicin against acute myeloid leukemia. *Drug Deliv.* 24 (1), 882–890. doi:10.1080/10717544.2017.1333170
- Liu, J. F., Jang, B., Issadore, D., and Tsourkas, A. (2019). Use of magnetic fields and nanoparticles to trigger drug release and improve tumor targeting. *Wiley Interdiscip. Rev. Nanomedicine Nanobiotechnology*. 11 (6), e1571. doi:10.1002/wnan.1571
- Liu, Y., Li, S., Li, H., Hossen, M. A., Sameen, D. E., Dai, J., et al. (2021). Synthesis and properties of core-shell thymol-loaded zein/shellac nanoparticles by coaxial electrospray as edible coatings. *Mater. Des.* 212, 110214. doi:10.1016/j.matdes.2021.110214
- Lu, Q., Dai, X., Zhang, P., Tan, X., Zhong, Y., Yao, C., et al. (2018). Fe₃O₄@ Au composite magnetic nanoparticles modified with cetuximab for targeted magnetothermal therapy of glioma cells. *Int. J. Nanomedicine* 13, 2491–2505. doi:10.2147/IJN.S157935
- Maurer, V., Altin, S., Ag Seleci, D., Zarinwall, A., Temel, B., Vogt, P. M., et al. (2021). *In-vitro* application of magnetic hybrid niosomes: Targeted siRNA-delivery for enhanced breast cancer therapy. *Pharmaceutics* 13 (3), 394. doi:10.3390/pharmaceutics13030394
- Mehta, S., and Jindal, N. (2013). Formulation of Tyloxapol niosomes for encapsulation, stabilization and dissolution of anti-tubercular drugs. *Colloids Surfaces B Biointerfaces*. 101, 434–441. doi:10.1016/j.colsurfb.2012.07.006
- Mohammadian, F., Abhari, A., Dariushnejad, H., Nikanfar, A., Pilehvar-Soltanahmadi, Y., and Zarghami, N. (2016). Effects of chrysin-PLGA-PEG nanoparticles on proliferation and gene expression of miRNAs in gastric cancer cell line. *Iran. J. Cancer Prev.* 9 (4), e4190. doi:10.17795/ijcp-4190
- Mohammadian, F., Abhari, A., Dariushnejad, H., Zarghami, F., Nikanfar, A., Pilehvar-Soltanahmadi, Y., et al. (2016). Upregulation of Mir-34a in AGS gastric cancer cells by a PLGA-PEG-PLGA chrysin nano formulation. *Asian Pac. J. Cancer Prev.* 16 (18), 8259–8263. doi:10.7314/apjcp.2015.16.18.8259
- Mokhtari, R. B., Homayouni, T. S., Baluch, N., Morgatskaya, E., Kumar, S., Das, B., et al. (2017). Combination therapy in combating cancer. *Oncotarget* 8 (23), 38022–38043. doi:10.18632/oncotarget.16723
- Momekova, D. B., Gugleva, V. E., and Petrov, P. D. (2021). Nanoarchitectonics of multifunctional niosomes for advanced drug delivery. *ACS omega* 6 (49), 33265–33273. doi:10.1021/acsomega.1c05083
- Mou, X., Ali, Z., Li, S., and He, N. (2015). Applications of magnetic nanoparticles in targeted drug delivery system. *J. Nanosci. Nanotechnol.* 15 (1), 54–62. doi:10.1166/jnn.2015.9585
- Myat, Y. Y., Ngawhirunpat, T., Rojanarata, T., Opanasopit, P., Bradley, M., Patrojanasophon, P., et al. (2022). Synthesis of polyethylene glycol diacrylate/acrylic acid nanoparticles as nanocarriers for the controlled delivery of doxorubicin to colorectal cancer cells. *Pharmaceutics* 14 (3), 479. doi:10.3390/pharmaceutics14030479
- O'Leary, M. P., Warner, S. G., Kim, S.-I., Chaurasiya, S., Lu, J., Choi, A. H., et al. (2018). A novel oncolytic chimeric orthopoxvirus encoding luciferase enables real-time view of colorectal cancer cell infection. *Mol. Therapy-Oncolytics*. 9, 13–21. doi:10.1016/j.omto.2018.03.001
- Osaka, T., Nakanishi, T., Shanmugam, S., Takahama, S., and Zhang, H. (2009). Effect of surface charge of magnetite nanoparticles on their internalization into breast cancer and umbilical vein endothelial cells. *Colloids Surfaces B Biointerfaces*. 71 (2), 325–330. doi:10.1016/j.colsurfb.2009.03.004
- Pardakhty1, A., and Moazeni, E. (2013). Nano-niosomes in drug, vaccine and gene delivery: A rapid overview. *Nanomedicine J.* 1.
- Pérez-Herrero, E., and Fernández-Medarde, A. (2015). Advanced targeted therapies in cancer: Drug nanocarriers, the future of chemotherapy. *Eur. J. Pharm. Biopharm.* 93, 52–79. doi:10.1016/j.ejpb.2015.03.018
- Prabha, G., and Raj, V. (2016). Preparation and characterization of polymer nanocomposites coated magnetic nanoparticles for drug delivery applications. *J. Magnetism Magnetic Mater.* 408, 26–34. doi:10.1016/j.jmmm.2016.01.070
- Ramimoghaddam, D., Bagheri, S., and Abd Hamid, S. B. (2015). Stable monodisperse nanomagnetic colloidal suspensions: An overview. *Colloids Surfaces B Biointerfaces*. 133, 388–411. doi:10.1016/j.colsurfb.2015.02.003
- Rodrigues Pereira da Silva, L. C., do Carmo, F. A., Eurico Nasciutti, L., Zancan, P., Cunha Sathler, P., and Mendes Cabral, L. (2016). Targeted nanosystems to prostate cancer. *Curr. Pharm. Des.* 22 (39), 5962–5975. doi:10.2174/1381612822666160715131359
- Rolston, K. V. (2017). Infections in cancer patients with solid tumors: A review. *Infect. Dis. Ther.* 6 (1), 69–83. doi:10.1007/s40121-017-0146-1
- Salmani Javan, E., Lotfi, F., Jafari-Gharabaghlu, D., Mousazadeh, H., Dadashpour, M., and Zarghami, N. (2022). Development of a magnetic nanostructure for co-delivery of metformin and silibinin on growth of lung cancer cells: Possible action through leptin gene and its receptor regulation. *Asian Pac. J. Cancer Prev.* 23 (2), 519–527. doi:10.31557/APJCP.2022.23.2.519
- Samed, N., Sharma, V., and Sundaramurthy, A. (2018). Hydrogen bonded niosomes for encapsulation and release of hydrophilic and hydrophobic anti-diabetic drugs: An efficient system for oral anti-diabetic formulation. *Appl. Surf. Sci.* 449, 567–573. doi:10.1016/j.apsusc.2017.11.055
- Shahbazi, R., Jafari-Gharabaghlu, D., Mirjafary, Z., Saeidian, H., and Zarghami, N. (2023). Design and optimization various formulations of PEGylated niosomal nanoparticles loaded with phytochemical agents: Potential anti-cancer effects against human lung cancer cells. *Pharmacol. Rep.* 75, 442–455. doi:10.1007/s43440-023-00462-8
- Solowey, E., Lichtenstein, M., Sallon, S., Paavilainen, H., Solowey, E., and Lorberbaum-Galski, H. (2014). Evaluating medicinal plants for anticancer activity. *Sci. World J.* 2014, 721402. doi:10.1155/2014/721402
- Soltan, S., and Matin, M. M. (2011). Cancer stem cells and cancer therapy. *Tumor Biol.* 32, 425–440. doi:10.1007/s13277-011-0155-8
- Stiufuc, R., Iacovita, C., Nicoara, R., Stiufuc, G., Florea, A., Achim, M., et al. (2013). One-step synthesis of PEGylated gold nanoparticles with tunable surface charge. *J. Nanomater.* 2013, 1–7. doi:10.1155/2013/146031
- Su, G., Zhou, H., Mu, Q., Zhang, Y., Li, L., Jiao, P., et al. (2012). Effective surface charge density determines the electrostatic attraction between nanoparticles and cells. *J. Phys. Chem. C* 116 (8), 4993–4998. doi:10.1021/jp211041m
- Tavano, L., Vivacqua, M., Carito, V., Muzzalupo, R., Caroleo, M. C., and Nicoletta, F. (2013). Doxorubicin loaded magneto-niosomes for targeted drug delivery. *Colloids Surfaces B Biointerfaces* 102, 803–807. doi:10.1016/j.colsurfb.2012.09.019
- Thun, M. J., DeLancey, J. O., Center, M. M., Jemal, A., and Ward, E. M. (2010). The global burden of cancer: Priorities for prevention. *Carcinogenesis* 31 (1), 100–110. doi:10.1093/carcin/bgp263
- Tiwari, A., Saraf, S., Jain, A., Panda, P. K., Verma, A., and Jain, S. K. (2020). Basics to advances in nanotherapy of colorectal cancer. *Drug Deliv. Transl. Res.* 10 (2), 319–338. doi:10.1007/s13346-019-00680-9
- Valková, V., Ďuranová, H., Bilčíková, J., and Habán, M. (2021). Milk thistle (Silybum marianum): A valuable medicinal plant with several therapeutic purposes. *J. Microbiol. Biotechnol. Food Sci.* 2021, 836–843. doi:10.15414/jmbfs.2020.9.4.836-843
- Van Houten, B., Hunter, S. E., and Meyer, J. N. (2016). Mitochondrial DNA damage induced autophagy, cell death, and disease. *Front. Biosci. (Landmark Ed.)* 21, 42–54. doi:10.2741/4375
- Wang, J., Wang, F., Li, F., Zhang, W., Shen, Y., Zhou, D., et al. (2016). A multifunctional poly (curcumin) nanomedicine for dual-modal targeted delivery, intracellular responsive release, dual-drug treatment and imaging of multidrug resistant cancer cells. *J. Mater. Chem. B* 4 (17), 2954–2962. doi:10.1039/c5tb02450a
- Yang, J., Lee, H., Hyung, W., Park, S.-B., and Sjjom, H. (2006). Magnetic PECA nanoparticles as drug carriers for targeted delivery: Synthesis and release characteristics. *J. Microencapsul.* 23 (2), 203–212. doi:10.1080/02652040500435444
- Zaki, N. M. (2014). Augmented cytotoxicity of hydroxycamptothecin-loaded nanoparticles in lung and colon cancer cells by chemosensitizing pharmaceutical excipients. *Drug Deliv.* 21 (4), 265–275. doi:10.3109/10717544.2013.838808
- Zheng, X., Lu, J., Deng, L., Xiong, Y., and Chen, J. (2009). Preparation and characterization of magnetic cationic liposome in gene delivery. *Int. J. Pharm.* 366 (1–2), 211–217. doi:10.1016/j.ijpharm.2008.09.019